A MATHEMATICAL MODEL FOR AIR BRAKE SYSTEMS IN THE PRESENCE OF LEAKS

A Thesis

by

SRIVATSAN RAMARATHNAM

Submitted to the Office of Graduate Studies of
Texas A&M University
in partial fulfillment of the requirements for the degree of

MASTER OF SCIENCE

August 2008

Major Subject: Mechanical Engineering

A MATHEMATICAL MODEL FOR AIR BRAKE SYSTEMS IN THE PRESENCE OF LEAKS

A Thesis

by

SRIVATSAN RAMARATHNAM

Submitted to the Office of Graduate Studies of
Texas A&M University
in partial fulfillment of the requirements for the degree of

MASTER OF SCIENCE

Approved by:

Co-Chairs of Committee,	K. R. Rajagopal
	Swaroop Darbha
Committee Members,	Jay Walton
Head of Department,	Dennis O'Neal

August 2008

Major Subject: Mechanical Engineering

ABSTRACT

A Mathematical Model for Air Brake Systems in the Presence of Leaks. (August 2008)

Srivatsan Ramarathnam, B.E, PSG College of Technology

Co–Chairs of Advisory Committee: Dr. K. R. Rajagopal
Dr. Swaroop Darbha

This thesis deals with the development of a mathematical model for an air brake system in the presence of leaks. Brake systems in trucks are crucial for ensuring the safety of vehicles and passengers on the roadways. Most trucks in the US are equipped with S-cam drum brake systems and they are sensitive to maintenance. Brake defects such as leaks are a major cause of accidents involving trucks. Leaks in the air brake systems affect braking performance drastically by decreasing the peak braking pressures attained and also increasing the time required to attain the same, thereby resulting in longer stopping distances. Hence there is a need for detecting leaks in an air brake system.

In this thesis, a mathematical model for an air brake system in the presence of leaks is developed with a view towards developing an automatic leak detection system in the near future. The model developed here builds on an earlier research at Texas A&M University in which a "fault free" model of an air brake system is developed, i.e., a mathematical model of an air brake system that predicts how the pressure in the brake chamber evolves as a function of the brake pedal input when there are no leaks in the air brake system.In order to develop a model for an air brake system in the presence of leaks, one must characterize a "leak". A leak may be characterized by the location and its size. Since the pipes are short, the location of the leak does not

significantly affect the evolution in the brake pressure as much as its size. For this reason, "effective area" of the leak was chosen as a characteristic of the leak. It was estimated by fitting an empirical relation for leak with leak flow measurement data. The supply pressure and effective area of leak comprised the inputs to the model along with the displacement of the foot pedal (treadle valve plunger). The model was corroborated with the experimental data collected using the setup at Texas A&M University.

To my parents, my sister, my cousins Mahesh and Lakshmi.

ACKNOWLEDGMENTS

I would like to express my heartfelt gratitude to Dr. Rajagopal and Dr. Swaroop for agreeing to be my advisors. It is a great honor and privilege to work under their guidance. I fervently thank Dr. Walton for consenting to be a member of my thesis committee.

I want to extend my sincere thanks to Dr. Shankar Coimbatore for his assistance during my induction into this project. I also thank my colleague, Mr. Sandeep Dhar for his invaluable help. I would also like to acknowledge the technical and support staff at Texas A&M University, for their assistance.

TABLE OF CONTENTS

LIST OF TABLES

LIST OF FIGURES

FIGURE Page

CHAPTER I

INTRODUCTION

A. Overview

Air brake systems are used in heavy commercial vehicles like buses, straight trucks and combination vehicles such as tractor-trailers[1]. More than 85% of the commercial vehicles in the US are equipped with S-cam drum brakes[2]. Proper functioning of the brake system of a commercial vehicle is critical not only from the safety viewpoint of the vehicle itself, but also for other vehicles and passengers in traffic. Any accident involving a commercial vehicle results not only in economic loss of the goods transported but also loss of life.

As air brake systems are highly sensitive to maintenance, periodic maintenance and inspection procedures have to be strictly followed[3]. Accidents involving commercial vehicles rarely occur due to brake failures but occur frequently due to brake defects. Typical brake related defects include oversize drums, worn out brake linings, out-of-adjustment push rod strokes and leaks in the system. Statistics indicate[4], that truck tractors pulling semi-trailers accounted for 63% of the trucks involved in fatal crashes and about 47% of the trucks involved in non fatal crashes. About 25% of the crashes involving trucks is due to brake deficiency and brake deficiency accounted for 39% of the total one-vehicle crashes.

Out-of-adjustment push rod strokes drastically decrease the maximum braking force that can be attained. This results in increased stopping distances, causing a safety hazard[5]. Leaks affect the brake system by reducing the peak braking pressures achieved in the brake chamber and also increasing the time for the pressure to build

---

The journal model is *IEEE Transactions on Automatic Control.*

up. Audible signs for leaks and/or immersing the pipes in water and looking for bubbles are two ways of detecting and locating leaks[6].

Most of the performance tests and visual based inspection tests of the air brake system indirectly correlate pressure in the brake chamber with the torque output, brake pad temperature, push rod strokes etc[7], [8]. More recently Shankar et al. [9] proposed a model for predicting the pressure transients in the brake chamber(in the absence of any defects) of a brake system. The treadle valve is treated as a nozzle and the dynamics are simulated with the treadle valve plunger displacement (brake pedal displacement) as input.

This thesis deals with the development of a mathematical model for predicting pressure transients in the brake chamber in the presence of leaks and the experimental corroboration of the same. An outline of the thesis is provided in the following section.

B. Organization of this thesis

- Chapter II is a brief overview of a typical air brake system found in commercial vehicles.
- Chapter III is a description about the experimental facility at Texas A&M University. A detailed explanation of the setup used to corroborate the mathematical model will be provided.
- Chapter IV is a description of the mathematical model for leaks in the system. A detailed explanation of the assumptions involved along with the methodology adopted will be presented.
- Chapter V presents the discussion of results and the future scope of the current work.

CHAPTER II

AIR BRAKE SYSTEM

Commercial vehicles utilize compressed air as a medium for transferring energy transfer during braking. A passenger car uses a hydraulic braking system, where a brake fluid is employed to transmit the muscular force of the driver[10]. A truck may haul anywhere between 20 to 30 times the weight of a passenger car. To generate braking forces required to stop a truck, a hydraulic brake system will not be commercially viable.

A. Layout of an air brake system

A typical brake system layout for a tractor trailer is presented in Fig.1[11]. The air brake system layout is also called as a dual brake circuit. The braking circuit is designed in such a way that, in case of a failure of one of the circuits, partial braking is possible with the help of the other. The two circuits are highlighted in green and orange colours in Fig.1. Some of the major components of an air brake system are described below:

1. **Compressor and reservoirs**: The compressor is the energy source for the whole braking system. The compressor is driven by the engine crankshaft through belt drives or gears. Compressed air is stored in the reservoirs. Typical operating pressures of the brake system are around 8 to 10 bars (100psig to 130psig). The reservoirs are equipped with a purge valve to drain moisture and contaminants. The reservoirs also have safety valves to prevent excessive pressure build up. A low pressure switch is also installed in the reservoir to warn the driver whenever the pressure in reservoirs drop below 65 psig. Compressed

air is generally passed through air filter, air dryer units to remove moisture and contaminants, so that clean air is fed to the system.

2. **Brake valve/Treadle valve**: The brake valve (also known as the treadle valve) is the heart of the braking system. Air supplied from the reservoirs is controlled and modulated by the brake valve and supplied to the brake chambers. The brake valve has a primary circuit and a secondary circuit. The primary circuit is actuated by the driver's foot on the brake pedal. Compressed air is supplied to brakes mounted on the rear axles through a relay valve. The secondary circuit is actuated by the primary circuit and supplies air to brakes on the front axle through a quick release valve. A typical brake valve and schematic of operation is shown in Fig.2[11].

3. **Quick release and relay valves**: A quick release valve (indicated as QR-1 in Fig.1) is used to quickly exhaust the air from front brake chambers once the brake pedal is released by the driver. A relay valve (indicated as R-12 valve in Fig.1) is used to actuate the rear brakes at the same time as the front brakes. Both the primary circuit of the brake valve and the supply from the reservoir are connected to the relay valve. Once the air from brake valve reaches the relay valve, a vent is opened to connect the supply reservoir to the rear brakes. Hence any delay in the travel of air from brake valve to the rear axles is eliminated by the relay valve eventhough the brake valve is located close to the front axles.

4. **Drum brakes**: S-cam drum brakes are the most commonly used brake configuration in commercial vehicles. They are also commonly referred as foundation brakes as they perform the actual braking function in the system. The drum brakes are mounted on the drive shaft of the axles. A typical drum brake assembly is illustrated in Fig.3[5].

5. **Brake chambers**: Brake chambers are used to convert the air pressure to braking force through the push rods. Pressure builds up in the brake chamber and results in the forward motion of the push rod, which rotates the automatic slack adjuster connected to it. The slack adjuster in turn, rotates the S-cam shaft tube and the S-cam, thereby expanding the brake linings to contact the drum. Brake chambers on the rear brakes are also called as spring brake chambers as parking brakes are also incorporated into them. A typical front (top) and rear brake chamber (bottom) is illustrated in Fig.4[11].

6. **Automatic slack adjusters**: A slack adjuster is designed to serve two functions. Firstly, the linear motion of the push rod is converted to rotational motion of the S-cam by the slack adjuster. Typically, out of adjustment push rods can be easily identified if the angle between the push rod and the slack adjuster is more than 90° during a brake application. Secondly, the clearance between the brake drum and the brake linings is maintained as the linings get worn out. Unlike a manual slack adjuster, an automatic slack adjuster does not require manual rotation of the adjuster nut for maintaining the lining to drum clearance. The construction of a typical automatic slack adjuster and its arrangement with the brake chamber is illustrated in Fig.5 and Fig.6[5].

For a complete and detailed description of all the components, their specifications, working principles, maintenance and testing details of the air brake system, the reader is requested to refer [11], [5] and [6].

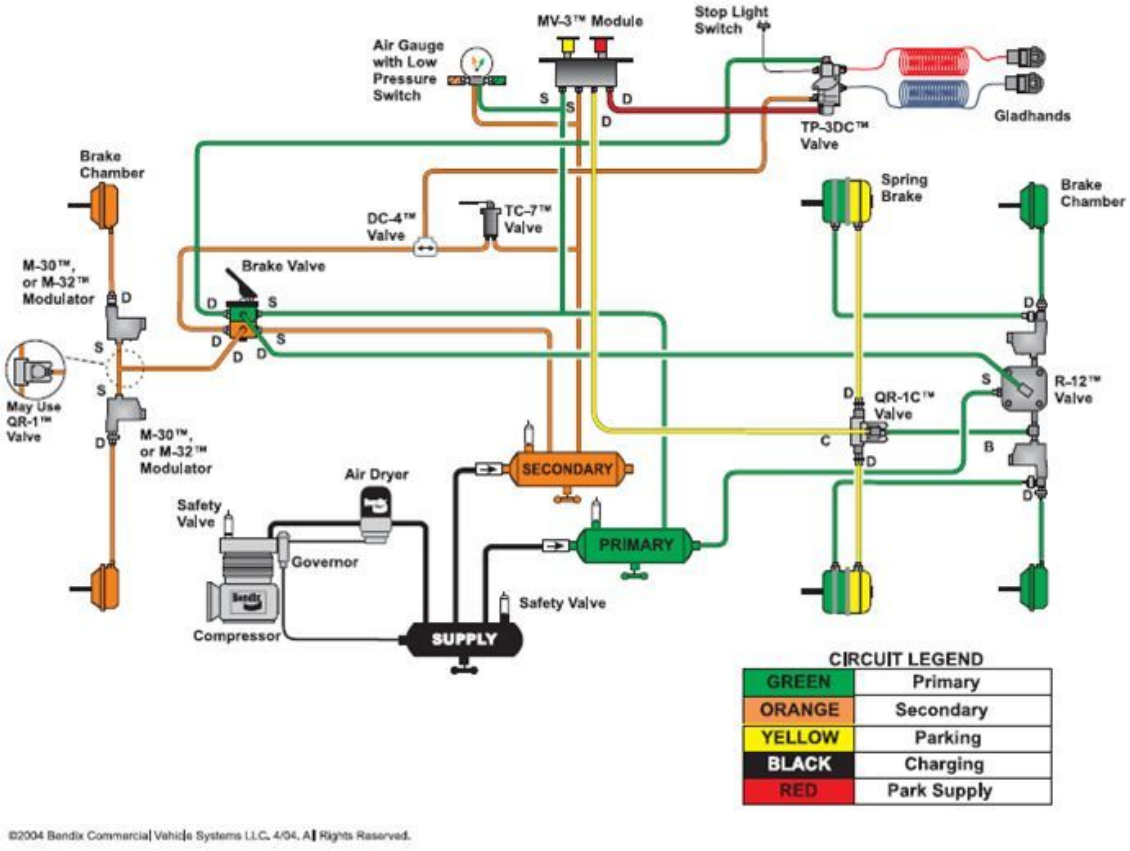

Fig. 1. Layout of an air brake system.

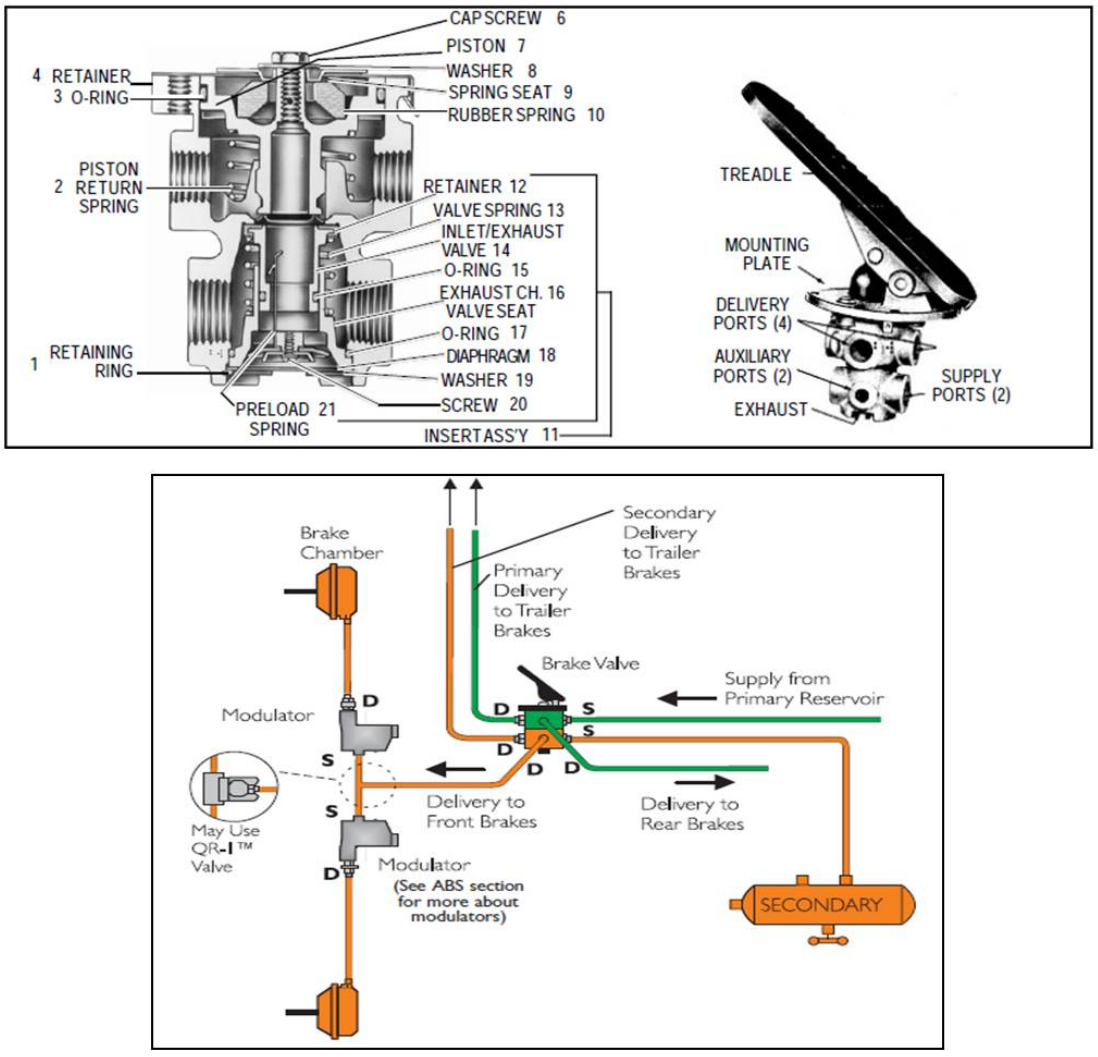

Fig. 2. Typical brake valve and schematic of operation.

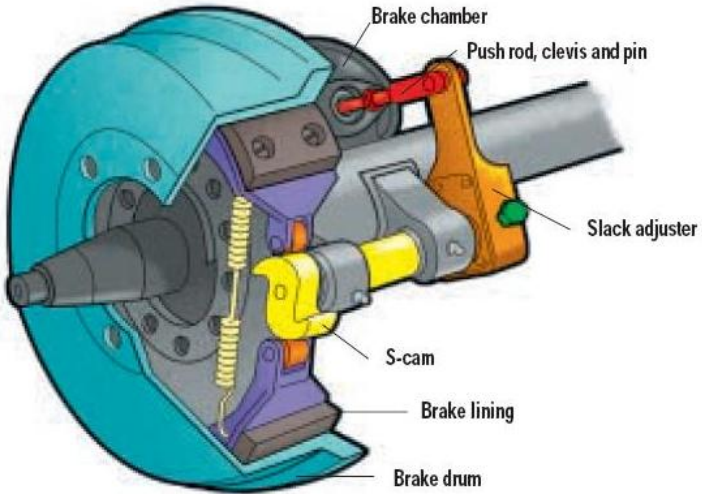

Fig. 3. A typical drum brake assembly.

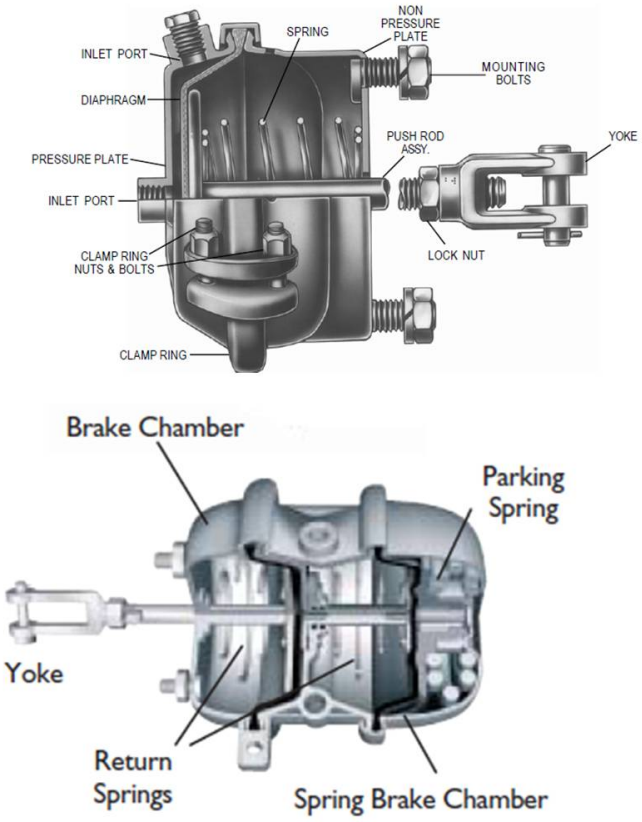

Fig. 4. Front and rear brake chambers.

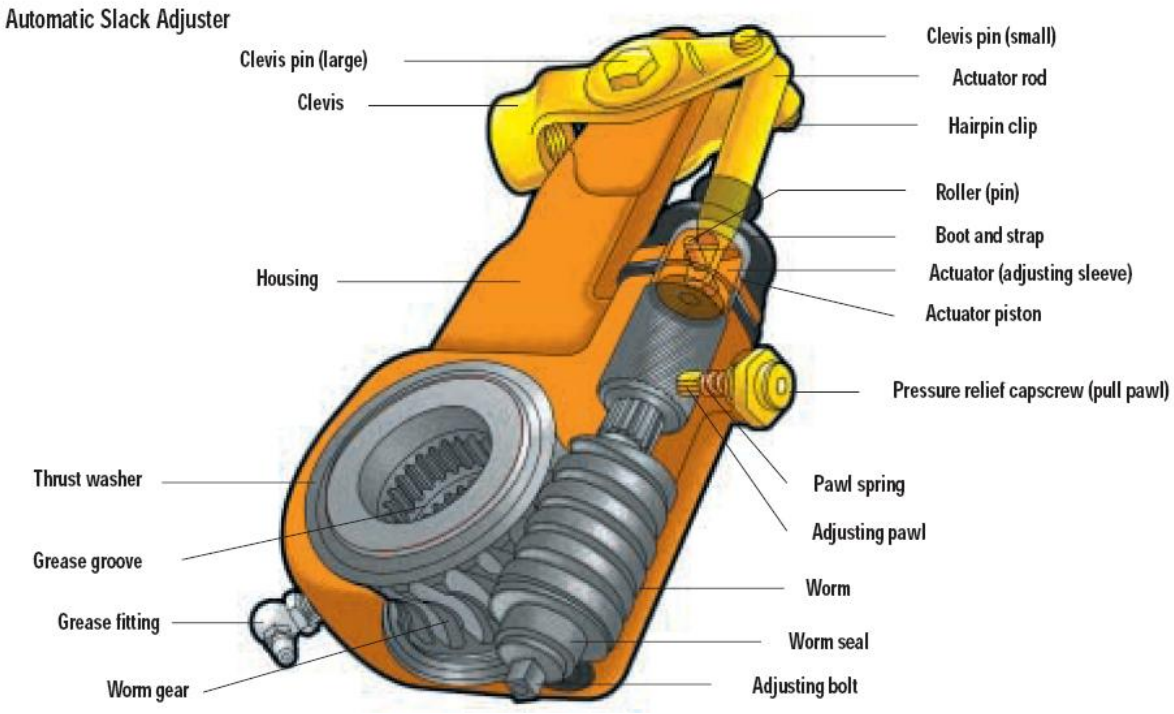

Fig. 5. Automatic slack adjuster construction.

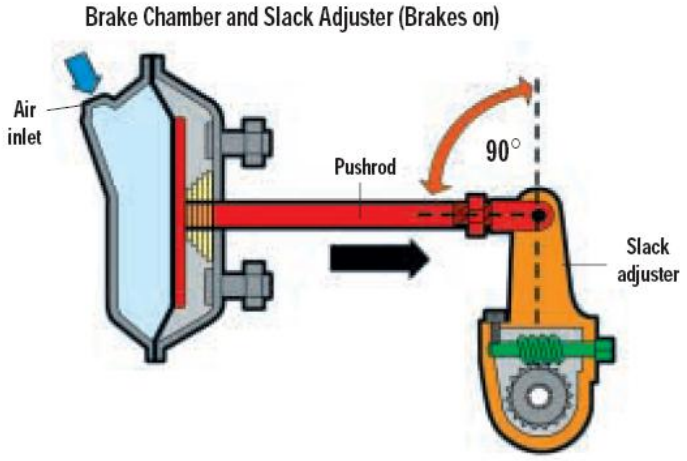

Fig. 6. Automatic slack adjuster and brake chamber.

CHAPTER III

EXPERIMENTAL SETUP

An experimental setup that closely resembles the actual air brake system in a commercial vehicle was built at Texas A&M University. A representative sketch of the experimental setup is shown in Fig.7[12].

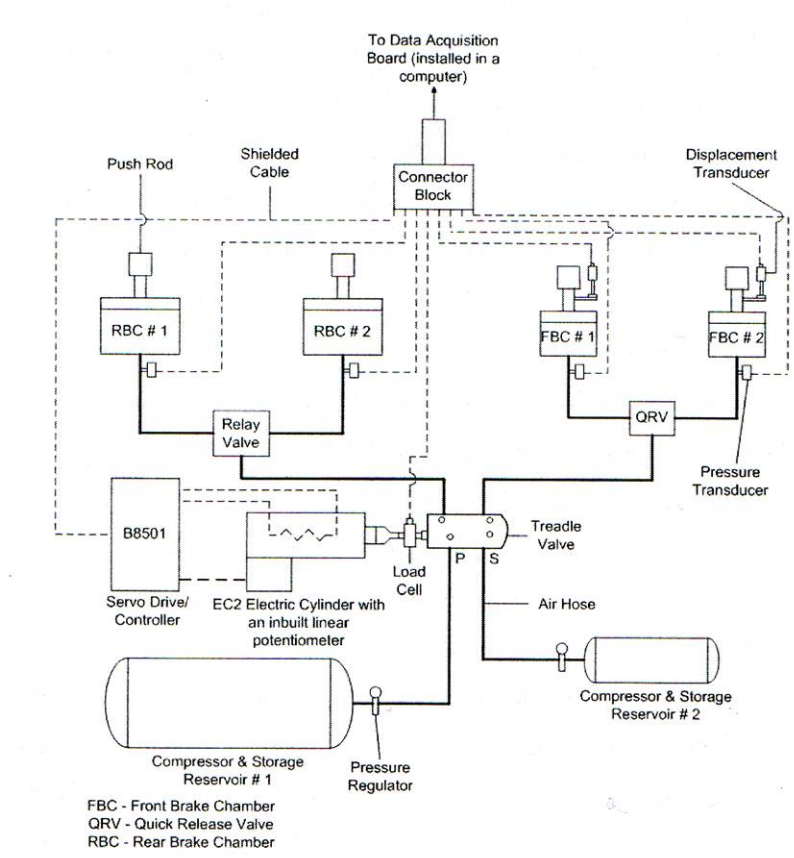

Fig. 7. Schematic of the experimental setup.

A. Details of the setup

The setup has two "Type-20" brake chambers on the front axle brakes and two "Type-30" brake chambers mounted on a fixture designed to simulate a rear axle. Air

is supplied by a 5HP air compressor and a 15 gallon storage reservoir. Pressure regulators are installed at the delivery side of the reservoir to control the air pressure supplied to the system. A dual brake valve (treadle valve) serves as the heart of the braking system.

One of the delivery ports of the treadle valve (called the primary delivery) is connected to the control port of the relay valve and the relay valve is, in turn, connected to the two rear brake chambers. Air supply from the reservoir is connected to the relay valve to complete the primary circuit. The other delivery port of the treadle valve (called the secondary delivery) is connected to the quick release valve (QRV) and in turn to the two front brake chambers. This is called the secondary circuit. During normal braking conditions, the primary circuit is actuated by the force exerted by the driver on the brake pedal. Compressed air delivered by the primary circuit then actuates a relay piston in the treadle valve which in turn actuates the secondary circuit.

The treadle valve was actuated using an electromechanical actuator with position feedback. The actuator was controlled by a servo drive/controller. Pressure transducers were mounted at the entrance of all brake chambers to record the pressure transients. A displacement transducer was mounted on each of the front brake chamber push rods to record the push rod stroke. All the sensors were interfaced using a Data Acquisition (DAQ) card mounted on a PC for data collection during the test runs. The desired treadle valve plunger motion was input from the computer to the servo drive through the DAQ card. A MATLAB/Simulink application was used to record and analyze the data. A complete description of all the foundation brake, actuation and data acquisition components of the setup can be found in [12].

B. Setup for measurement of leak

For the purpose of measuring a leak in the air flow, a graduated Flow Control Valve (FCV) manufactured by Mead Fluid Dynamics[13], was installed to obtain a greater control over the degree of leak introduced in the system. Four turns on the dial of the FCV completely opened the valve. The primary delivery of the treadle valve is directly connected to one of the front brake chambers for all test runs. The FCV is installed between the primary delivery and the brake chamber as shown in Fig.8. Leaks of varying degrees are introduced by turning the dial of the FCV by half-a-turn, one full turn, two full turns etc.

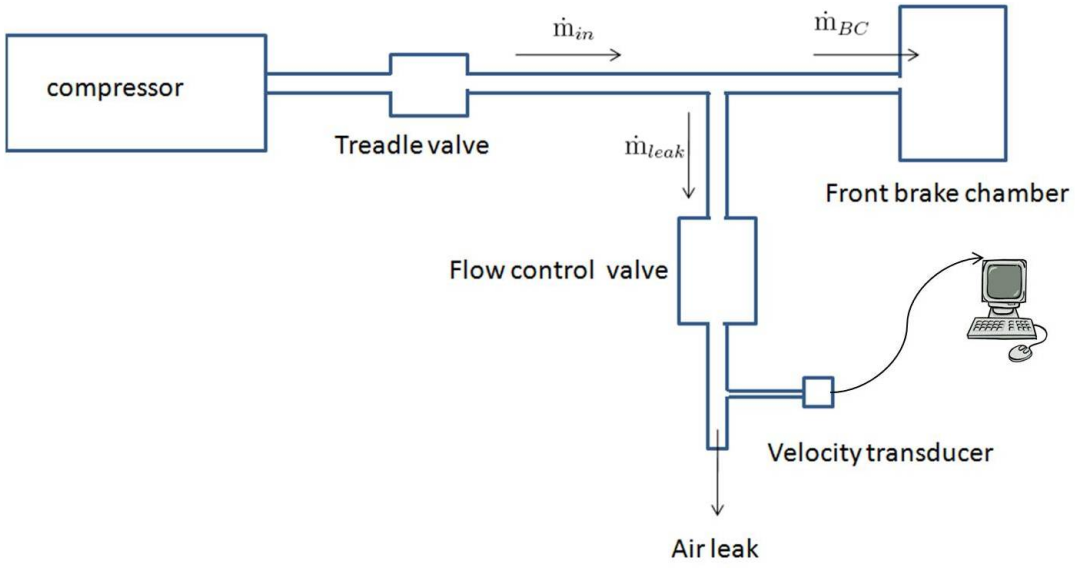

Fig. 8. Schematic of the leak measurement setup.

To measure the mass flow rates of the air leaking out from the system, a velocity transducer manufactured by All Sensors Corporation[14], was installed. The sensor was interfaced using the DAQ card and the voltage outputs were recorded during the test runs. The voltage outputs from the sensor were then converted to dynamic pressure using the calibration curve of the sensor. This pressure data was then converted to velocity and in turn to mass flow rate. A few photographs of the experimental setup can be seen Fig.9 through Fig.14.

Fig. 9. Air brakes system laboratory.

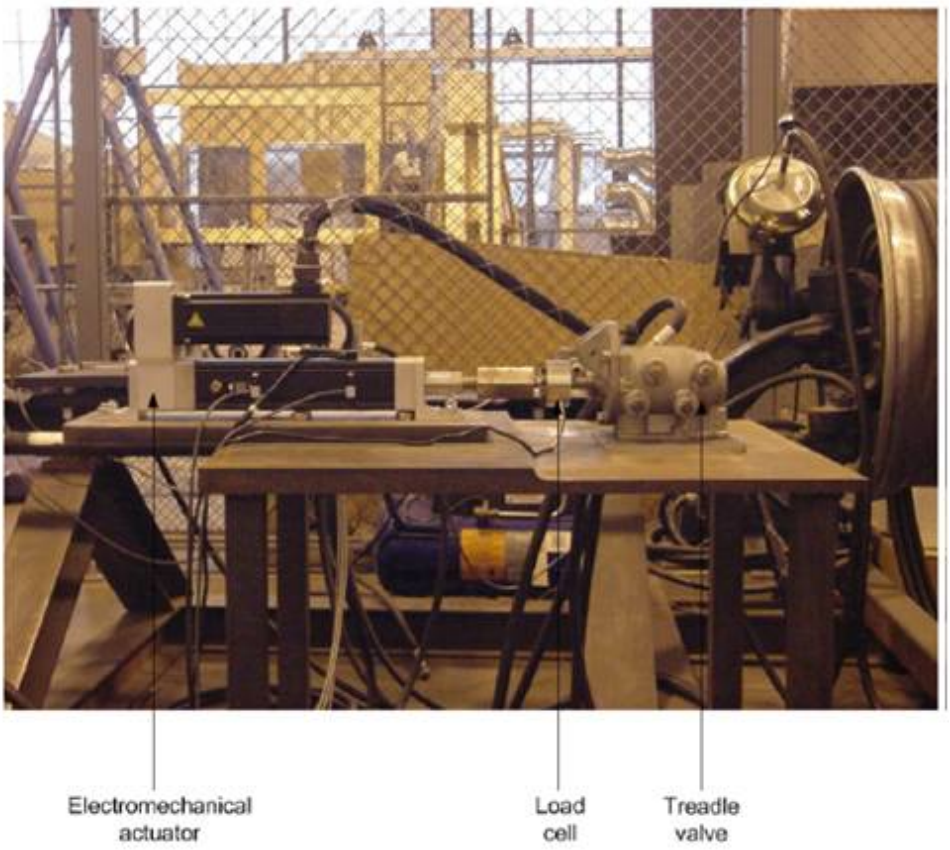

Fig. 10. Front axle assembly.

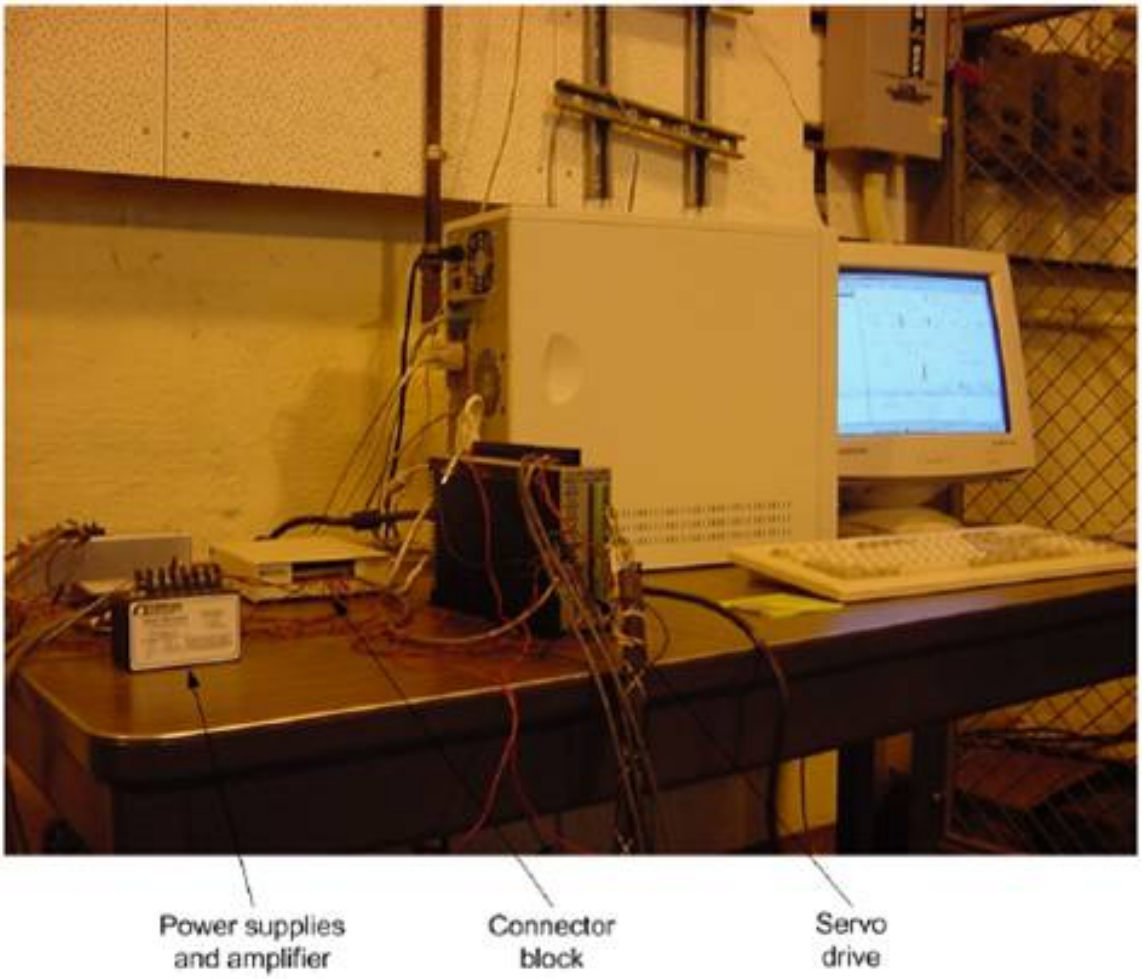

Fig. 11. Data acquisiton system.

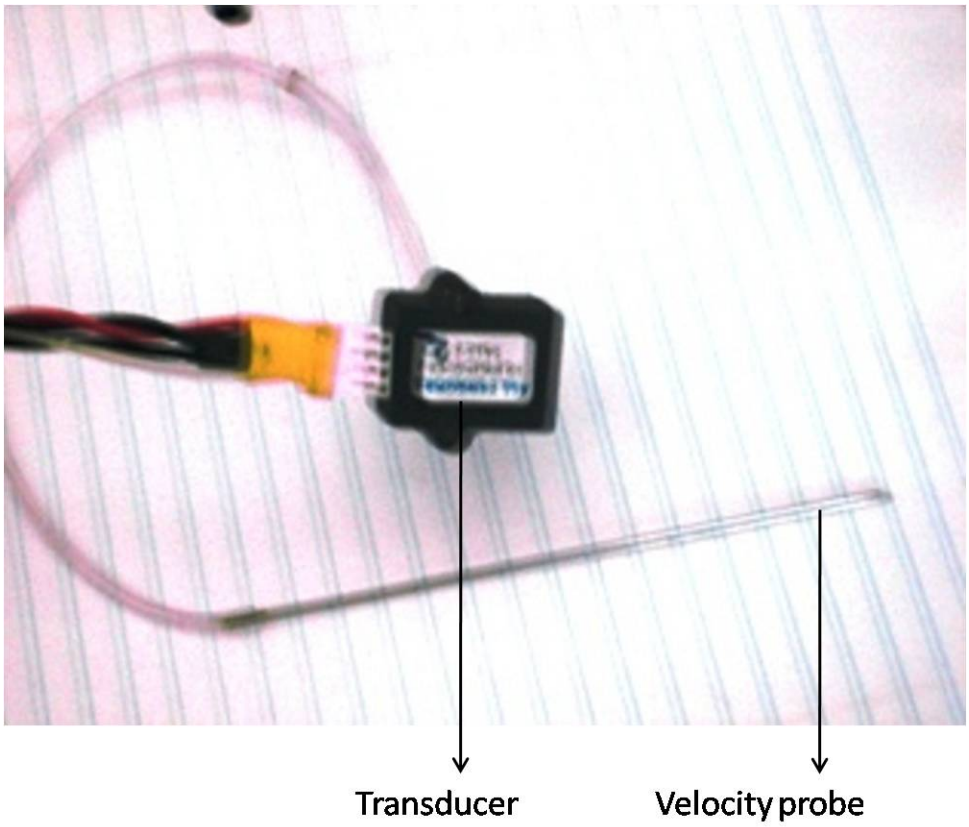

Fig. 12. Velocity transducer.

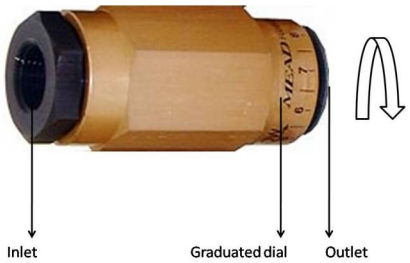

Fig. 13. Flow control valve.

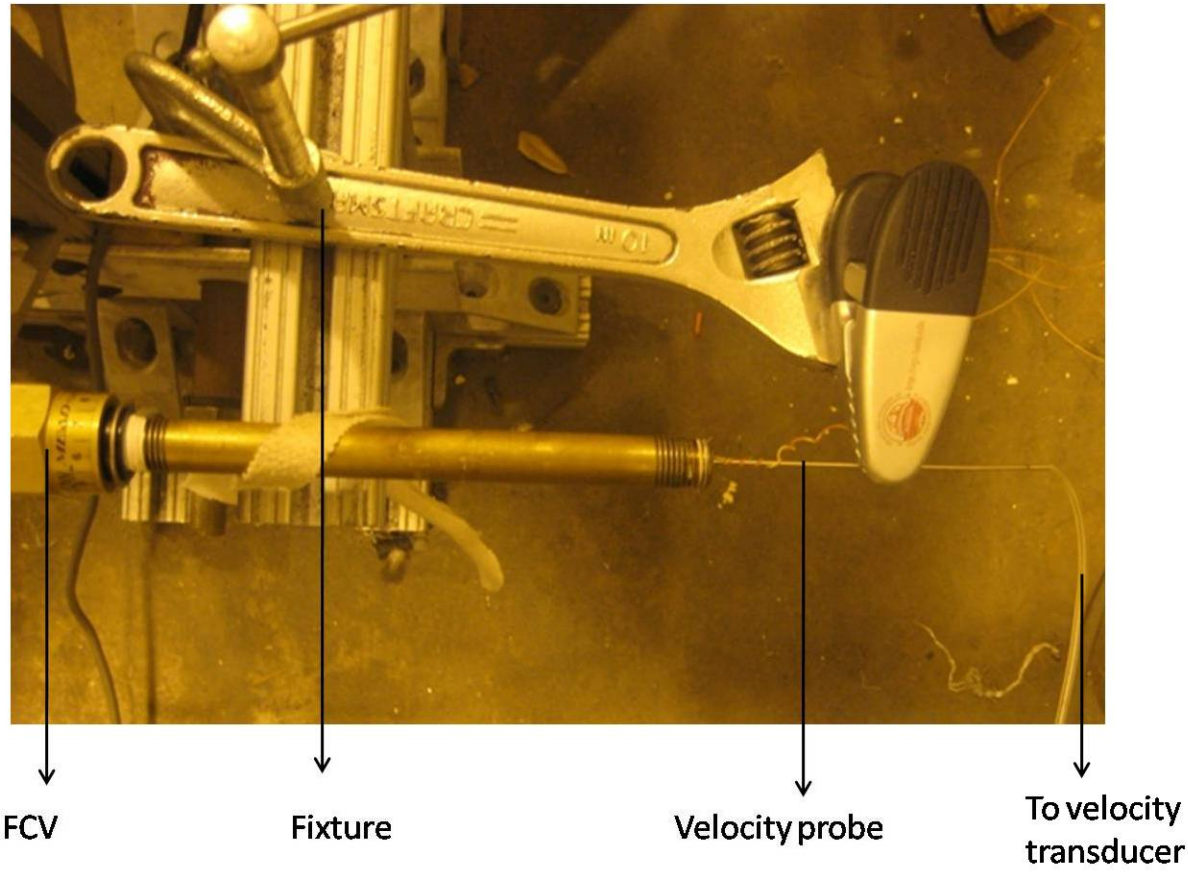

Fig. 14. Leak measurement setup.

CHAPTER IV

A MATHEMATICAL MODEL FOR LEAK

This section deals with, the methodology for developing a mathematical model in the presence of leaks. A brief description of the "fault-free" model developed in [12] follows as it forms the building block for the mathematical model that is desired.

A. "Fault-free" model

As the name suggests, the "fault-free" model is one that predicted the pressure response of the brake system in the absence of any faults or defects such as leaks etc. This model correlated the pressure in the brake chamber with the treadle valve plunger displacement and the supply pressure to the system. The model was developed for a brake system configuration where, one of the front brake chambers was directly connected to the primary delivery port of the treadle valve. A lumped parameter approach was employed.

1. Assumptions

The governing equations of the "fault-free" model was developed using the following assumptions:

1. Friction at all sliding surfaces of the valves was assumed insignificant since all components were very well lubricated.
2. Inertial forces were found to be infinitesimally small compared to the pressure forces and spring forces.
3. The primary inlet valve opening of the treadle valve was assumed to behave like a nozzle.

4. Properties in the supply chamber of the treadle valve were assumed to be the stagnation properties for the inlet of the nozzle.

5. Flow through the treadle valve opening was assumed to be one-dimensional and isentropic.

6. Air was assumed to behave like an ideal gas with constant specific heats.

7. Uniform fluid properties were assumed at all sections in the nozzle. Also, the peak Mach number of the compressed air flow in the system was measured and found to be less than 0.2.

For a complete list of assumptions involved in the development of the governing equations, the reader is encouraged to refer [12].

2. Governing equations

Governing equations for characterizing the pressure response of the brake systems were obtained, by an extended application of balance of mass and energy for the pneumatic subsystem as shown in Fig.15[12].

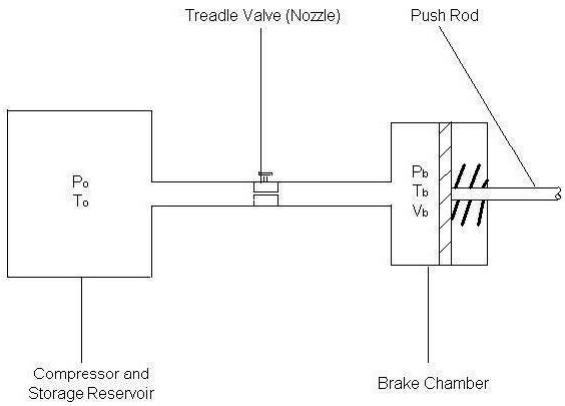

Fig. 15. Schematic of the pneumatic subsystem.

The set of governing equations developed were

$$= \begin{cases} \left(\frac{2\gamma}{(\gamma-1)RT_0} \left[\left(\frac{P_b}{P_0}\right)^{\frac{2}{\gamma}} - \left(\frac{P_b}{P_0}\right)^{\frac{\gamma+1}{\gamma}} \right]^{\frac{1}{2}} \right) A_p C_D P_o \text{sgn}(P_o - P_b) \\ \left(\frac{V_{o1} P_0^{\frac{\gamma-1}{\gamma}}}{\gamma RT_0 P_0^{\frac{\gamma-1}{\gamma}}} \right) \dot{P}_b & \text{if } P_b < P_{th} \\ \left(\frac{V_b P_0^{\frac{\gamma-1}{\gamma}}}{\gamma RT_0 P_0^{\frac{\gamma-1}{\gamma}}} + \frac{P_b^{\frac{1}{\gamma}} A_b M_1 P_0^{\frac{\gamma-1}{\gamma}}}{RT_0} \right) \dot{P}_b & \text{if } P_{th} \leq P_b < P_{ct} \\ \left(\frac{V_b P_0^{\frac{\gamma-1}{\gamma}}}{\gamma RT_0 P_0^{\frac{\gamma-1}{\gamma}}} + \frac{P_b^{\frac{1}{\gamma}} A_b M_1 P_0^{\frac{\gamma-1}{\gamma}}}{RT_0} \right) \dot{P}_b & \text{if } P_b \geq P_{ct} \end{cases} \quad (4.1)$$

For a detailed derivation, variables involved and their nomenclature, the reader is requested to refer [9].

3. Features of the "fault-free" model

From the above equations, following inferences can be made[12]:

1. There are three modes for the pressure evolution. In the first mode, pressure increases to a threshold limit. Once the threshold is crossed, the push rods extend and the brake shoes contacts the brake drum, making the system transfer to second mode. Once the brake shoes contact the drum, system goes to the third mode and the pressure increases to reach a steady state value.

2. The governing equation in each mode is a nonlinear first order ordinary differential equation.

3. The governing equation for each mode is different.

4. The system shifts from one mode to another based upon the transition conditions, which are linear inequalities.

The above set of equations were solved using the fourth order Runge-Kutta numerical method to obtain the pressure response in the brake chamber. Treadle

valve plunger displacement was the input to the numerical scheme. The model was corroborated with several experimental measurements and the results can be found in [9].

B. Modeling the leak

The "fault-free" model discussed above, predicted the pressure transients reasonably well if there were no leaks in the system as shown in Fig.16[12].

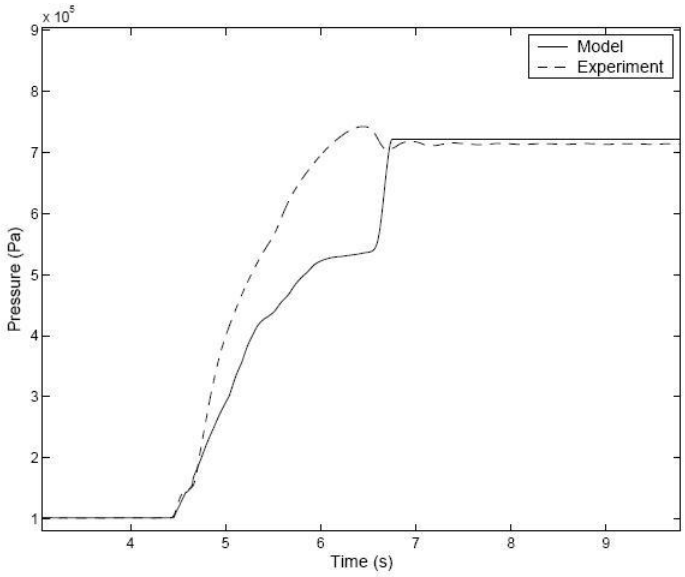

Fig. 16. Pressure transients at 722 kPa (90 psi) supply pressure with no leak.

Modeling the pressure transients in the presence of leaks will help in comparing the rise times for pressure evolution with the norms specified by FMVSS[15]. Estimation of stopping distances from brake torque measurements require the rise time for pressure build up, which can be obtained from such models.

1. Problem definition

The governing equations are developed for a brake system configuration considered in the "fault-free" model (a front brake chamber directly connected to the primary delivery of the treadle valve) . The leak is assumed to be near the brake chamber and after the treadle valve as shown in Fig.8. Site of the leak is assumed to behave like a nozzle. Since air leaks to the atmosphere, and since the ratio of supply pressure to atmospheric pressure is greater than the critical pressure ratio [16], choked flow conditions are assumed. By conservation of mass,

$$\dot{m}_{in} - \dot{m}_{leak} = \dot{m}_{BC} \tag{4.2}$$

where, the total mass flow rate from the treadle valve is denoted by $\dot{m}_{in}$, the mass flow rate of air leaked to atmosphere is denoted by $\dot{m}_{leak}$ and the mass flow rate of air entering the brake chamber is denoted as $\dot{m}_{BC}$. Since there were no leaks or losses in the system, mass balance for the "fault-free" model is

$$\dot{m}_{in} = \dot{m}_{BC} \tag{4.3}$$

The expression for $\dot{m}_{in}$ is the expression found on the left hand side of Eq.4.1 and is given by

$$\dot{m}_{in} = \left(\frac{2\gamma}{(\gamma-1)RT_0} \left[\left(\frac{P_b}{P_0} \right)^{\frac{2}{\gamma}} - \left(\frac{P_b}{P_0} \right)^{\frac{\gamma+1}{\gamma}} \right]^{\frac{1}{2}} \right) A_p C_D P_o \text{sgn}(P_o - P_b) \tag{4.4}$$

The right hand side of Eq.4.1 is the expression for $\dot{m}_{BC}$ for various modes and is given by

$$\dot{m}_{BC} = \begin{cases} \left(\frac{V_{o1} P_0^{\frac{\gamma-1}{\gamma}}}{\gamma R T_0 P_0^{\frac{\gamma-1}{\gamma}}} \right) \dot{P}_b & \text{if } P_b < P_{th} \\ \left(\frac{V_b P_0^{\frac{\gamma-1}{\gamma}}}{\gamma R T_0 P_0^{\frac{\gamma-1}{\gamma}}} + \frac{P_b^{\frac{1}{\gamma}} A_b M_1 P_0^{\frac{\gamma-1}{\gamma}}}{R T_0} \right) \dot{P}_b & \text{if } P_{th} \leq P_b < P_{ct} \\ \left(\frac{V_b P_0^{\frac{\gamma-1}{\gamma}}}{\gamma R T_0 P_0^{\frac{\gamma-1}{\gamma}}} + \frac{P_b^{\frac{1}{\gamma}} A_b M_1 P_0^{\frac{\gamma-1}{\gamma}}}{R T_0} \right) \dot{P}_b & \text{if } P_b \geq P_{ct} \end{cases} \tag{4.5}$$

For the model to capture effects of leak, an expression for $\dot{m}_{leak}$ needs to determined and subtracted from $\dot{m}_{in}$. The resulting expression would then be equated to $\dot{m}_{BC}$ of Eq.4.1. The underlying logic is that a portion of air from the treadle valve is leaked out and the remaining quantum of air enters the brake chamber giving rise to the pressure transients.

2. Derivation of $\dot{m}_{leak}$

It was observed during the experiments, that the mass flow rate of leak increased with the supply pressure and also with the area of leak (determined by number of turns of the FCV). The influence of location of the leak on the pressure evolution was not significant. Hence $\dot{m}_{leak}$ may be assumed to be of the form

$$\dot{m}_{leak} = f(P_{sup}, A_l) \tag{4.6}$$

where, P_{sup} is the supply pressure and A_l is the area of leak. In reality, area of the leak, A_l ,may not be known a priori. Yet it has to be incorporated into the model as it is one of the input variables along with supply pressure, P_{sup}. We will assume the following constitutive relationship for the mass flow rate of leaking air:

$$\dot{m}_{leak} = C_d A_l \frac{P_{sup}}{\sqrt{RT}} \sqrt{\left(\frac{2}{\gamma+1}\right)^{\left(\frac{\gamma+1}{\gamma-1}\right)}} \tag{4.7}$$

where, C_d is coefficient of discharge, γ is the ratio of specific heats for air, R is the universal gas constant for air. We will define K as:

$$K = \frac{C_d A_l}{\sqrt{R}} \sqrt{(\frac{2}{\gamma+1})^{(\frac{\gamma+1}{\gamma-1})}} \tag{4.8}$$

so that

$$\dot{m}_{leak} = \frac{K P_{sup}}{\sqrt{T}}. \tag{4.9}$$

The term $C_d A_l$ will be referred to as "effective leak area" since the actual leak area is not known. From (4.8), $C_d A_l$ is easily obtained as

$$C_d A_l = \frac{K\sqrt{R}}{\sqrt{(\frac{2}{\gamma+1})^{(\frac{\gamma+1}{\gamma-1})}}} \tag{4.10}$$

Once $C_d A_l$ is determined, it is input to the leak expressions(4.7) and (4.2). The methodology adopted to determine $C_d A_l$ is described in the subsequent subsection.

3. Estimating the effective leak area

As mentioned before, area of the leak may not be known in reality. A leak may result from loose connections/couplings, kinked hoses or defective valve ports etc.

In this section, we will use a least squares approach to determine the effective area of the leak[17]. Since we can measure the mass flow rate of leaking air, the supply pressure and the temperature (of air leaking out), we can determine the value of K that minimizes the least squares error given below:

$$err = \sum_{i=1}^{N} (\dot{m}_{meas}(i) - K\frac{P_{sup}(i)}{\sqrt{T}})^2 \tag{4.11}$$

where, N is the total number of samples, i is the sample number, $\dot{m}_{meas}$ is the measured leak mass flow rate. Parameter K was found for leak measurements performed at different supply pressures (90 psi, 80 psi etc) and at different FCV settings (half-a-

turn, single turn, two turns etc) . The corresponding effective leak area, $C_d A_l$ is then immediately obtained from (4.10).

C. Experimental procedure

Several leak measurements were performed to collect the mass flow rates of leak during a full brake application. For a given supply pressure, say 90 psi, leaks were introduced in the system in steps of half-a-turn until two-and-a-half turns of the FCV. This was repeated for other supply pressures say 80 psi, 70 psi etc.

1. Corroboration of measurements

A series of experiments were conducted to corroborate the leak flow measurements prior to the actual leak measurements in the brake system. The compressor delivery was directly connected to the FCV. For each leak setting, the compressor was allowed to drain completely. Since the DAQ card could collect data continuously for only 60 seconds[18], the experiments were conducted as follows.

Compressor was allowed to drain for 60 seconds at a particular FCV setting. FCV was closed at the end of 60 seconds. Steady state compressor delivery pressure was noted at the start and also at the end of the 60 second interval. Data was collected from the velocity transducer continuously for the 60 second period. This was repeated at the same FCV setting till all the air in the reservoir was drained out. A schematic of the setup is given in Fig.17.

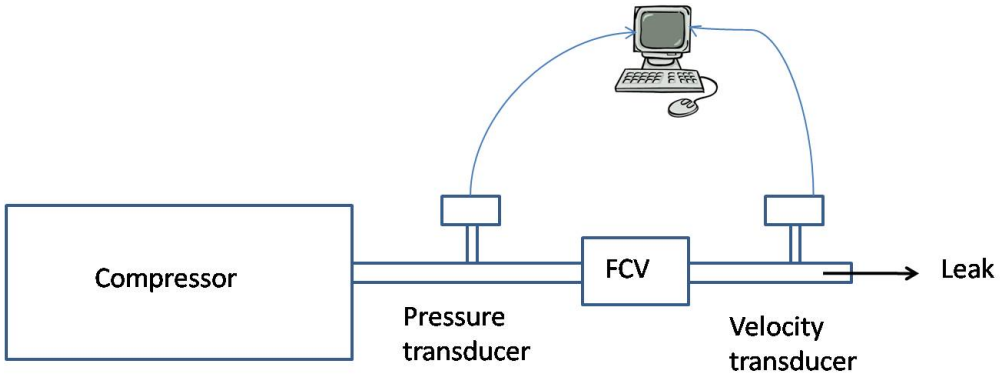

Fig. 17. Schematic of the setup for leak corroboration tests.

Since the leak flow is very turbulent, average velocity of flow was computed from the measured velocity using the"one-seventh"power law approximation of velocity profiles[19], [20]. The ratio of average velocity to the measured centerline velocity was found to be

$$\frac{\overline{V}}{U} = \frac{2n^2}{(n+1)(2n+1)} \tag{4.12}$$

where, $\overline{V}$ is the average velocity, U is the measured centerline velocity, n is a constant and is equal to 7. The average velocity $\overline{V}$ is utilized for all the mass flow rate calculations.

From the mass flow rates calculated using (4.11), the total amount of air leaked from the compressor was found by integrating the mass flow rates with respect to time. This was compared with the values predicted by the ideal gas equation. Multiple runs were conducted to test for repeatability of measurements. The measured values were found to be in close agreement. Comparison of one such run performed at one turn of FCV is presented in Fig.18.

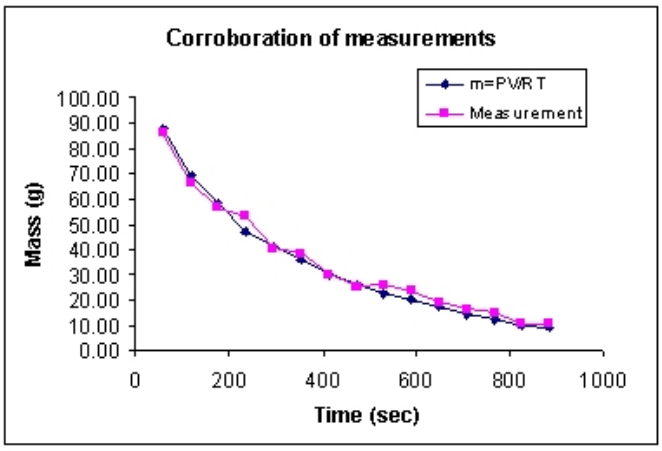

Fig. 18. Comparison of measured and predicted mass values at two turns of FCV.

2. Leak measurements

After the corroboration experiments, the desired leak measurement experiments were performed using the setup described in Fig.8. The measured leak mass flow rates are tabulated in Tables.I, II, III and IV.

Table I. Leak mass flow rates for a full brake application at 90 psi supply pressure

Supply pressure (psi)	No. of turns of FCV	mass flow rate (g/s)
90	0.5	0.83
	1	1.18
	1.5	1.60
	2	1.82
	2.5	2.35
	3	5.21

Table II. Leak mass flow rates for a full brake application at 80 psi supply pressure

Supply pressure (psi)	No. of turns of FCV	mass flow rate (g/s)
80	0.5	0.74
	1	1.10
	1.5	1.40
	2	1.66
	2.5	2.06
	3	5.18

Table III. Leak mass flow rates for a full brake application at 70 psi supply pressure

Supply pressure (psi)	No. of turns of FCV	mass flow rate (g/s)
70	0.5	0.61
	1	0.84
	1.5	1.17
	2	1.42
	2.5	1.62
	3	4.80

Table IV. Leak mass flow rates for a full brake application at 60 psi supply pressure

Supply pressure (psi)	No. of turns of FCV	mass flow rate (g/s)
60	0.5	0.55
	1	0.75
	1.5	1.05
	2	1.19
	2.5	1.50
	3	3.81

It can be easily inferred from Fig.19, that there is a sudden jump in the mass flow rates of air leaked out between 2.5 turns and 3 turns of the FCV. Leaks greater than three turns of the FCV resulted in very small pressure build up in the brake chamber. This is shown in Fig.20 and Fig.21. Such large leaks were not considered since warning devices for such occurrences are already in place. Moreover, the schemes we are developing for small leaks are expected to provide warnings well in advance that one would not be in such a situation. Therefore, only "small leaks" (upto 2.5 turns of FCV) are taken into consideration. Thus, these mass flow rates were input into the leak flow models to estimate K, $C_d A_l$ and the pressure transients were obtained in the presence of leak. Since FMVSS norms[15] dictate that all leak tests be done at full brake application and at a reservoir pressure of 90 psi, results for this supply pressure will be presented and discussed in detail in the subsequent chapter.

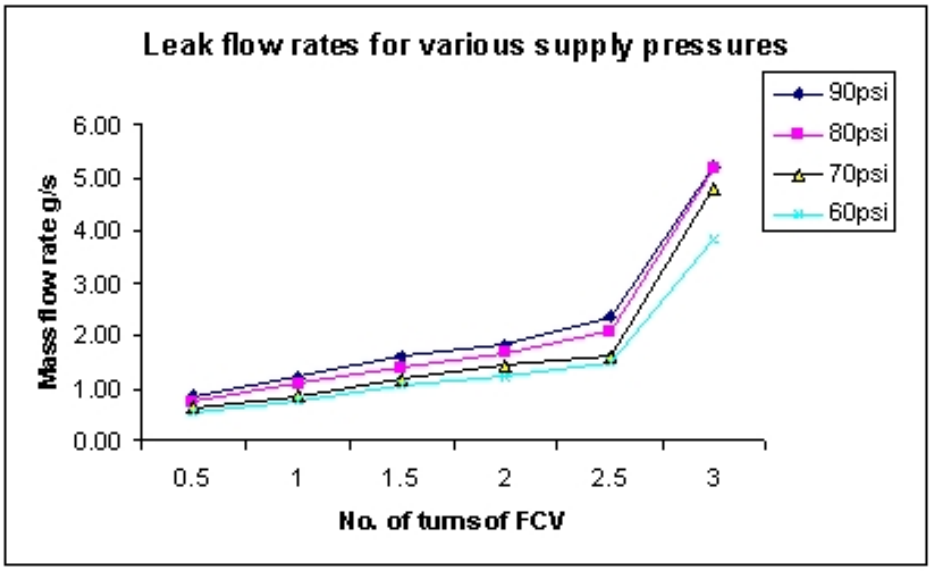

Fig. 19. Leak mass flow rates at various supply pressures and FCV settings.

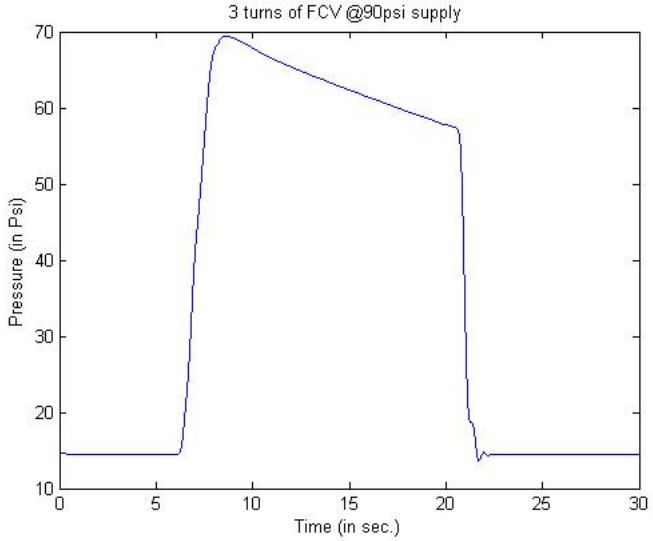

Fig. 20. Pressure transients at 90 psi supply and 3 turns of FCV.

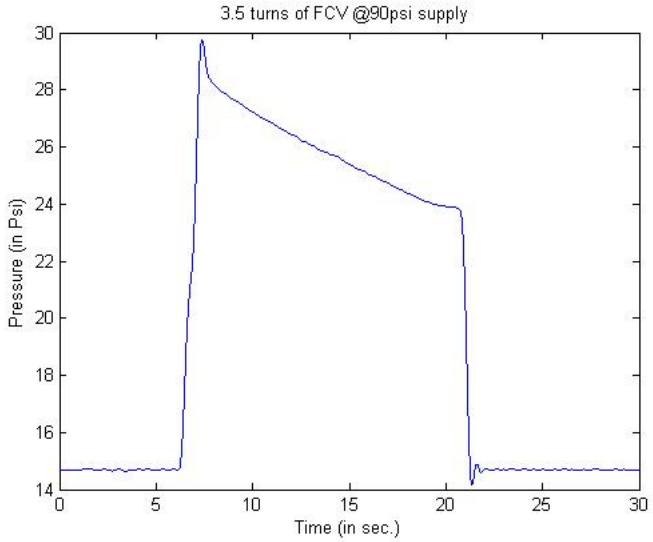

Fig. 21. Pressure transients at 90 psi supply and 3.5 turns of FCV.

CHAPTER V

RESULTS AND DISCUSSION

From the leak mass flow rates, the parameter K and C_dA_l are estimated and presented in Table.V. A key point to be noted is that C_dA_l doesn't represent the actual area of the leak i.e., the opening of the FCV. It is an"effective" area of leak. An effective area of 4.8e-6 m^2 may be visualized as an equivalent circular aperture of a diameter of 2.5mm[17]. The effective areas of leak for corresponding FCV settings are then input

Table V. Estimates of K and effecive leak area

Supply pressure (psi)	No. of turns of FCV	K	C_dA_l (m^2)
90	0.5	1.940E-07	4.832E-06
	1	3.229E-07	8.045E-06
	1.5	4.779E-07	1.191E-05
	2	5.778E-07	1.440E-05
	2.5	7.646E-07	1.905E-05

into the leak flow model and the governing equations. The result of the simulations are compared with experimentally obtained measurements and are presented from Fig.22 to Fig.26. It can be easily seen that the model predicts the pressure transients in the presence of leaks very closely to the measured values. The difference between the model and the measured values are presented in Table.VI. P_{meas} is the experimentally measured steady state pressure. P_{model} is the steady state brake chamber pressure predicted by the model. Percentage error is defined as $\frac{P_{meas}-P_{model}}{P_{meas}} \times 100$. The model over predicts the experiment in the first two cases and under predicts for the last case. The model matches very closely the experimental results for FCV setting of 2 turns.

A. Summary of results

Table VI. Comparison of model and measured steady state pressures

Supply pressure (psi)	No. of turns of FCV	$P_{meas}(psi)$	$P_{model}(psi)$	$error\%$
90	0.5	87.28	89.58	-2.72
	1	86.76	89.00	-2.58
	2	85.78	86.53	-0.88
	2.5	85.53	84.07	1.71

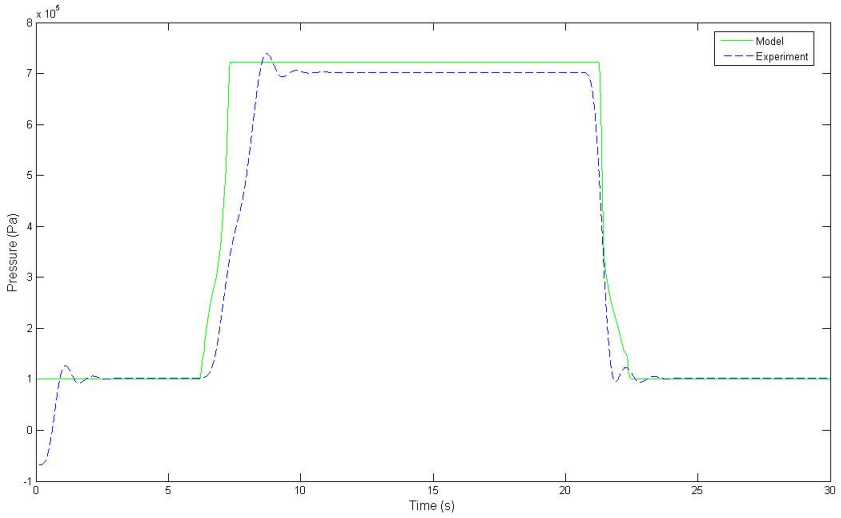

Fig. 22. Pressure transients at 90 psi supply and no leak.

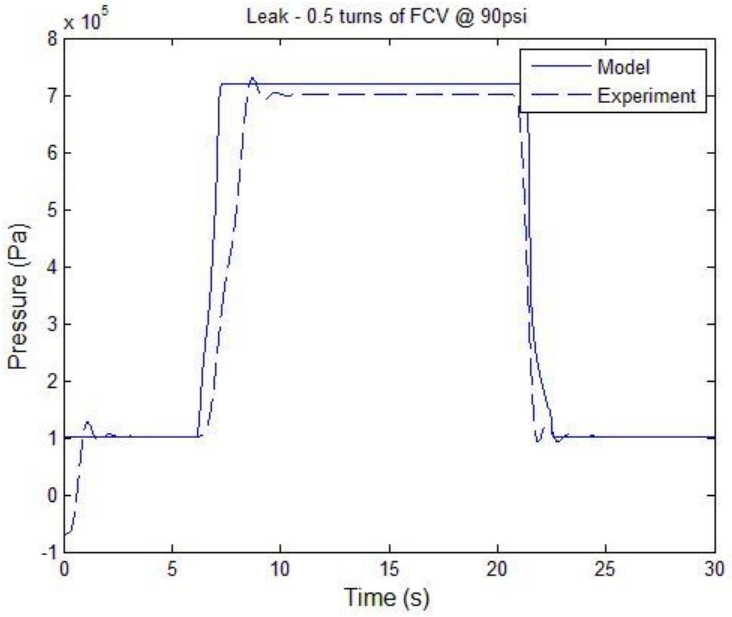

Fig. 23. Pressure transients at 90 psi supply and 0.5 turns of FCV.

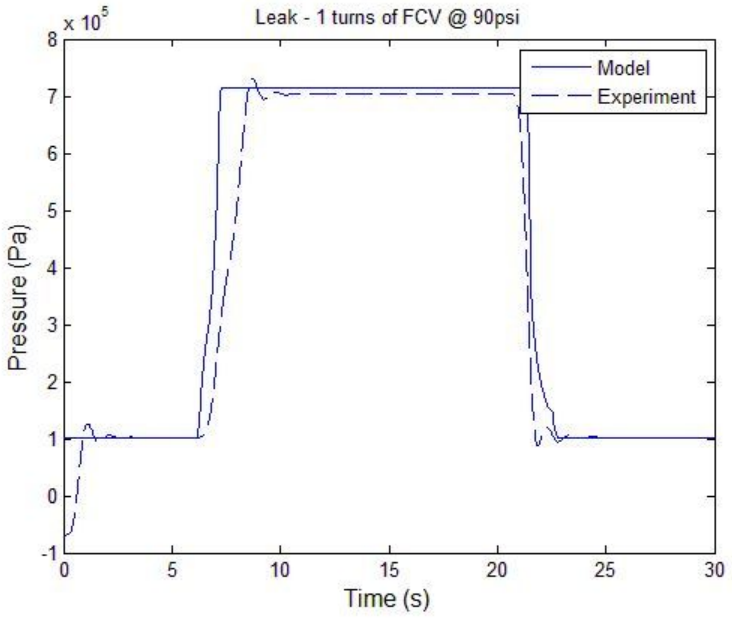

Fig. 24. Pressure transients at 90 psi supply and 1 turns of FCV.

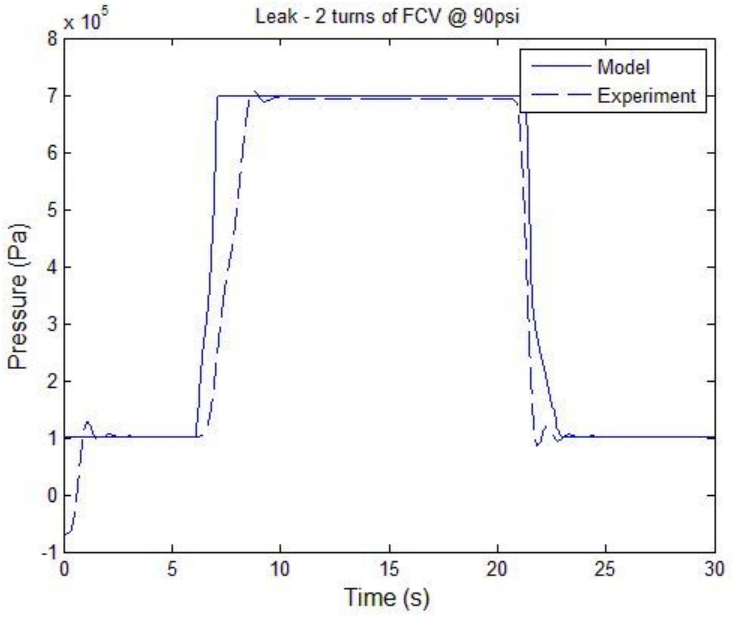

Fig. 25. Pressure transients at 90 psi supply and 2 turns of FCV.

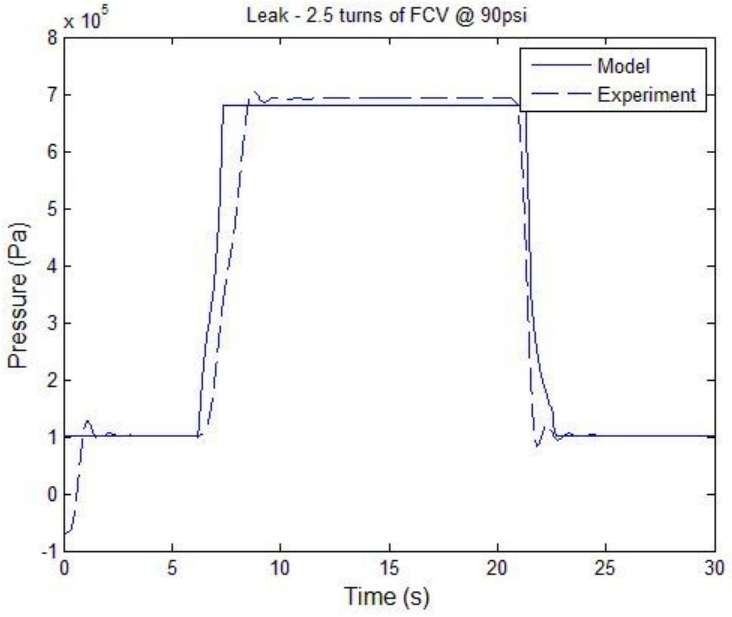

Fig. 26. Pressure transients at 90 psi supply and 2.5 turns of FCV.

From(4.8), it is expected that the parameter K and effective area of leak, C_dA_l have a linear relationship[17]. It turns out that K versus C_dA_l curve is indeed linear as shown in Fig.27.

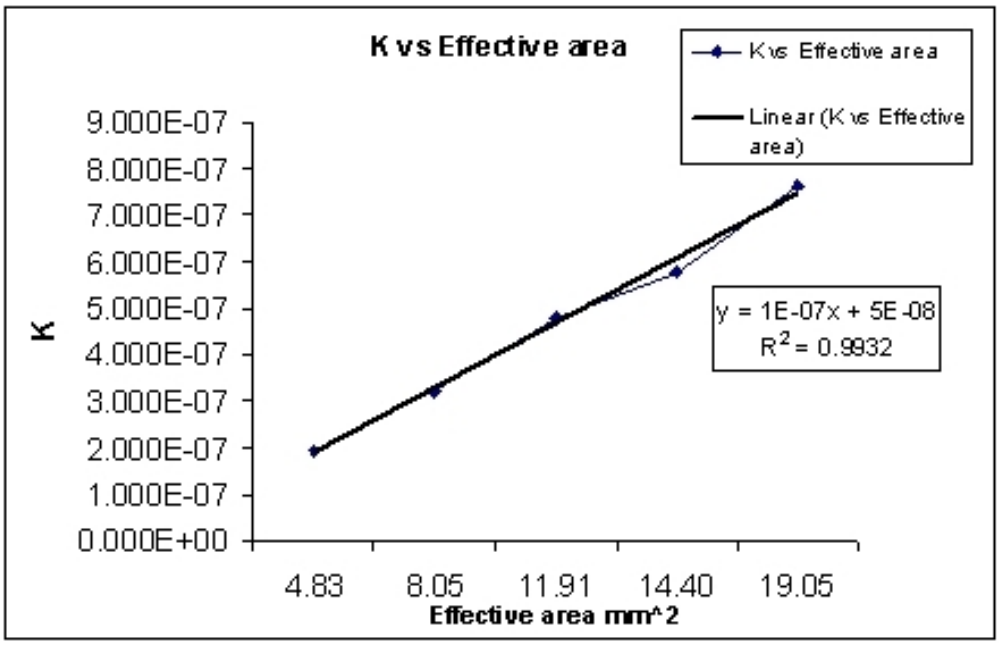

Fig. 27. K versus effective area of leak.

B. "Realistic leaks"

To simulate realistic leaks, a set of flow control orifices[21] were installed instead of the FCV to introduce leaks. The orifices ranged from 0.4mm diameter to 1.6mm diameters. Experiments were run at full brake application with leak introduced through these orifices. In the case of real time leaks, the only diagnostic data available would be the measured steady state brake chamber pressure. Based on this value, one must be able to make a judgment whether there is leak in the system or not.

This can be done by comparing the steady state pressure attained during a test with the values obtained in Tables.I and VI. For example, let the measured steady

state pressure during a full brake application with 90 psi supply be 83 psi. Looking up Table.VI, it can be inferred that a leak is present whose magnitude is slightly greater than 2.5 turns of FCV (effective area $19mm^2$). To quantify it precisely, from Table.I, we can conclude that the severity of the leak is given by a leak flow rate greater than . Hence Tables.I to VI serve as a "master look-up"data for leaks.

In the case of the leak model, the measured steady state pressure is used to obtain the effective area of leak using the calibration curve,

$$C_d A_l = -2.4945 P_{ss} + 229.34 \tag{5.0}$$

where, $C_d A_l$ is in mm^2, P_{ss} is the measured steady state pressure in psi. This curve was obtained by plotting the steady state pressure values predicted by the model in Table.VI with the effective areas obtained from Table.V. An inverse linear relationship is observed between the steady state pressure and the effective area of leak, which is expected. This is shown in Fig.28. The estimated effective leak areas are summarized

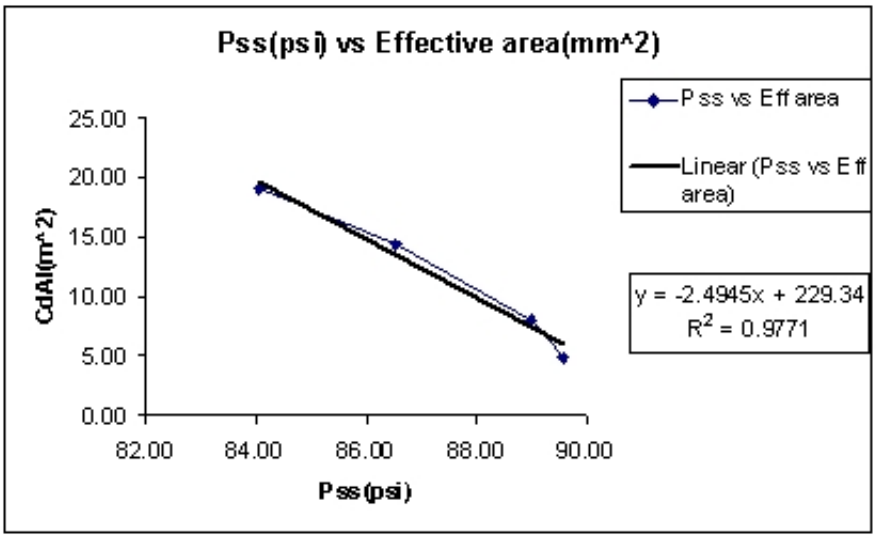

Fig. 28. Effective area of leak versus steady state pressure.

in Table.VII. Where, P_{sup} is the supply pressure and P_{ss} is the steady state pressure.

The C_dA_l, hence obtained is input to the leak model to predict the pressure transients. It is observed from Fig.29 to Fig.33 that the model predicts the pressure transients very closely to the experimentally obtained pressure data. From Tables.V and VII, it is noted that the effective area of leak for two turns of FCV and 1.4mm orifice are pretty close. Thus, it can be stated that the leak introduced by two turns of FCV is equivalent to the leak introduced by a 1.4mm orifice. From Table.I, the severity of this leak can be stated in terms of the mass flow rate of leak as 1.82 g/s.

Table VII. Estimates of K and effective leak area for the orifices

P_{sup} (psi)	Orifice dia (mm)	P_{ss}(psi)	K	$C_dA_l(mm^2)$
90	0.5	87.34	5.189E-08	11.47
	1.00	86.53	2.192E-07	13.48
	1.20	86.51	3.002E-07	13.55
	1.40	85.86	4.192E-07	15.16
	1.63	82.53	5.694E-07	23.46

C. Summary

A mathematical model for predicting the pressure transients in the brake chamber in the presence of leaks has been presented. Measurements of supply pressure, treadle valve plunger displacement and leak mass flow rates are utilized to develop the model. The model has been developed in compliance with current FMCSA and FMVSS norms for brake systems in commercial vehicles. All input data to the model are obtained during a full brake application with a supply pressure of 90 psi (722 kPa).

The brake system configuration investigated consisted a front brake chamber directly connected to the primary delivery port of the treadle valve. Controlled amounts of leak are introduced using a flow control valve. A “master” leak data set is obtained

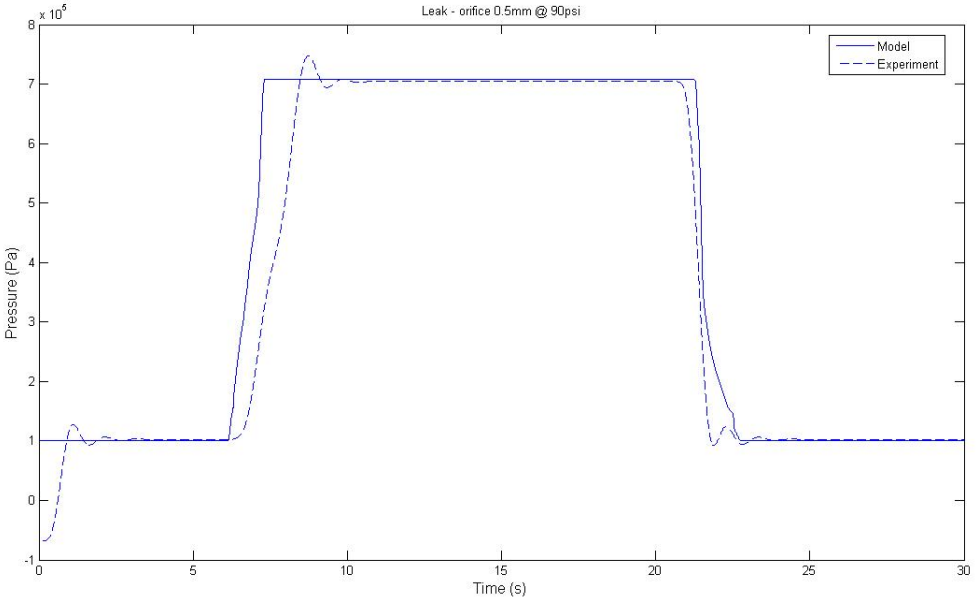

Fig. 29. Pressure transients at 90 psi supply with 0.5mm orifice.

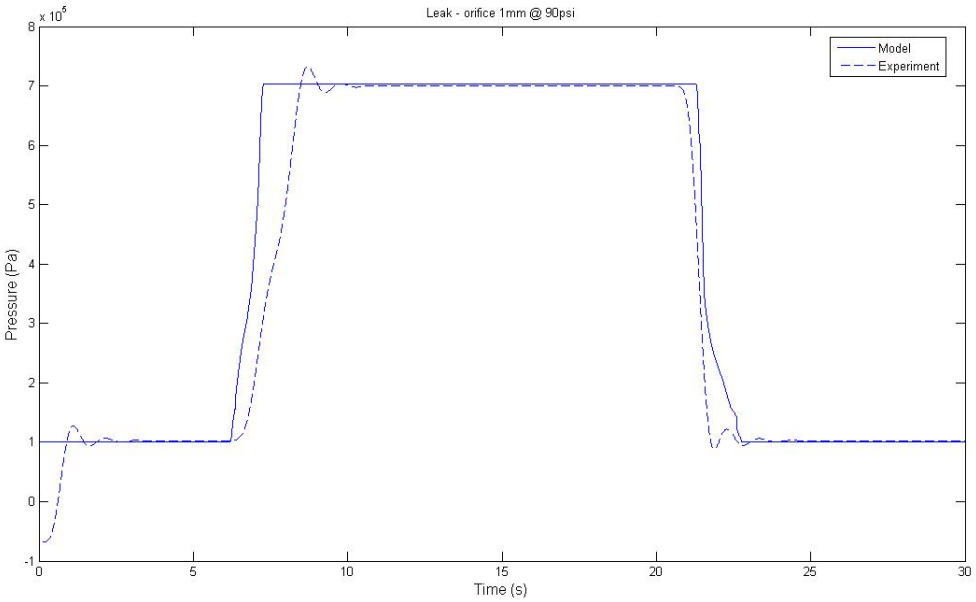

Fig. 30. Pressure transients at 90 psi supply with 1mm orifice.

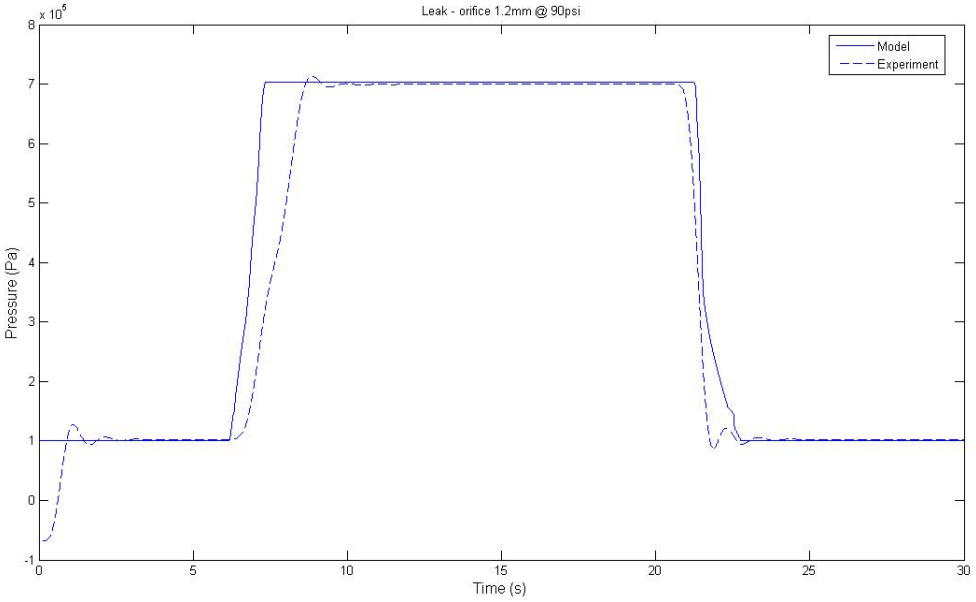

Fig. 31. Pressure transients at 90 psi supply with 1.2mm orifice.

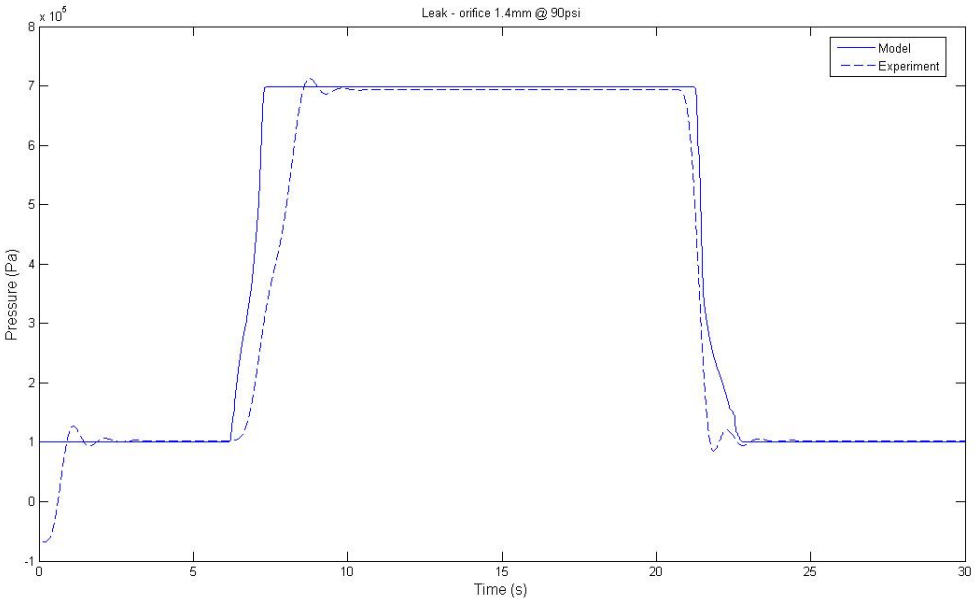

Fig. 32. Pressure transients at 90 psi supply with 1.4mm orifice.

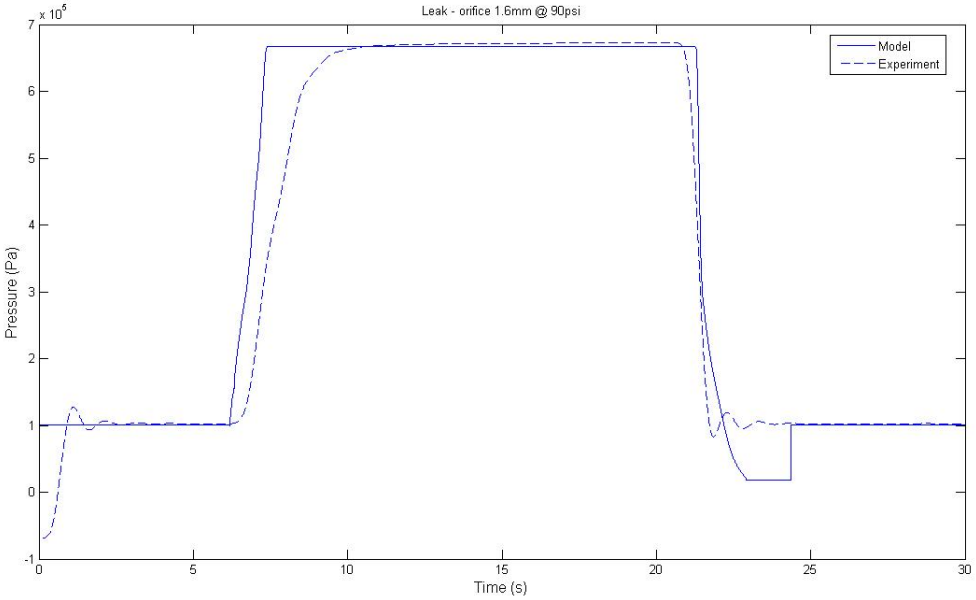

Fig. 33. Pressure transients at 90 psi supply with 1.6mm orifice.

with the help of leak flow measurements. An empirical relationship for mass flow rate of leak is developed with supply pressure and area of leak as independent variables. This empirical relation is fitted with the measurements and an"effective area" of leak is estimated. The effective area of leak and the empirical relation are then input to the previously developed "fault-free"model to obtain the pressure transients in the presence of leaks. To simulate "realistic" leaks, flow control orifices of known diameters were employed to introduce leaks in the system. From measured steady state pressures in the brake chamber, effective area of leak is estimated by "looking up" the "master" leak data set.

D. Scope of future work

It is hoped that the mathematical model developed be utilized to estimate push rod strokes in the presence of leaks. It is also hoped that the model for predicting leaks

and push rod strokes be developed for the whole truck or a tractor which can be incorporated into a fast and reliable portable diagnostic tool for inspecting air brake systems. Such a device will reduce inspection times, manpower and costs involved. In the long run, it is also hoped that the model take shape as a telematics based on-board diagnostic monitor for the brake systems.

1. Road (blocks) to the future

Some of the immediately foreseeable issues or challenges to be surmounted are listed below:

1. The mathematical model presented in this thesis is for a single front brake chamber connected directly to the primary delivery of the treadle valve. The model did not take into account the effects of relay valve, quick release valve and other brake system components.

2. The values of the parameters used in the model, (like brake chamber diaphragm area) are based on the configuration of the system used in the current experimental setup. Depending on whether the vehicle is a school bus, straight truck, multi-axle tractor or tractor-trailer(s) combination, the brake layout varies accordingly. Moreover, vehicle/component design varies from manufacturer to manufacturer. All these component to component, layout to layout variations need to be taken into account and the parameter values need to be incorporated accordingly.

3. Such an extensive model requires careful and rigorous corroboration using tests performed with the actual vehicle, since safety is of tantamount importance. Also, the diagnostic schemes need to be implemented in such a way that they are accurate, fast and computationally less intensive.

4. Both the "fault-free" model and the model developed in this thesis require the use of pressure transducers for measuring brake chamber pressure. In the current setup, a pressure transducer is mounted at the entry of every brake chamber. Such transducers don't exist in current generation commercial vehicles. A tractor-semitrailer combination vehicle may require ten such transducers.

5. It is hoped that as telematics and on-board diagnostics gain more prominence and economic viability, incorporation of pressure transducers and interfacing to the vehicle's Electronic Control Unit (ECU) will not be a major bottle-neck.

REFERENCES

[1] Robert Bosch GmbH., *Automotive Brake Systems*, Society of Automotive Engineers (SAE), Warrendale, PA, 1995.

[2] S.F. Williams and R.R. Knipling, "Automatic slack adjusters for heavy vehicle air brake systems," *Research Report DOT HS*, vol. 807, pp. 724, 1991.

[3] FMCSA, "Minimum periodic inspection standards," [Online]. Available: http://www.fmcsa.dot.gov/rules-regulations/administration/fmcsr/appng.htm, accessed May 2008.

[4] USDOT-FMCSA, "The large truck crash causation study," [Online]. Available: http://www.ai.volpe.dot.gov/ltccs/default.asp?page=reports, accessed May 2008.

[5] New Brunswick Department of Public Safety, "Air brake manual," [Online]. Available: http://www.gnb.ca/0276/vehicle/pdf/ab_manual-e.pdf, accessed May 2008.

[6] Texas Department of Public Safety, "Texas commercial motor vehicle drivers' handbook," [Online]. Available: http://www.txdps.state.tx.us/ftp/forms/CDLhandbook.pdf, accessed May 2008.

[7] S.J. Shaffer and G.H. Alexander, "Commercial Vehicle Brake Testing–Part 1: Visual Inspection Versus Performance-Based Test," SAE International, Warrendale, PA, 1995.

[8] S.J. Shaffer and G.H. Alexander, "Commercial Vehicle Brake Testing–Part 2: Preliminary Results of Performance-Based Test Program," SAE International, Warrendale, PA, 1995.

[9] S.C. Subramanian, S. Darbha, and K.R. Rajagopal, "Modeling the pneumatic subsystem of an S-cam air brake system," *Journal of Dynamic Systems, Measurement, and Control*, vol. 126, pp. 36, 2004.

[10] H. Heisler, *Vehicle and Engine Technology 2nd ed.*, SAE International, Warrendale, PA, 1999.

[11] Bendix, "Air brake manual," [Online]. Available: http://www.bendixvrc.com/itemDisplay.asp?documentID=5032, accessed May 2008.

[12] S.C. Subramanian, "A diagnostic system for air brakes in commercial vehicles," Ph.D. dissertation, Texas A&M University, College Station, Texas, 2006.

[13] Mead Fluid Dynamics, "Dyla-trol flow controls," [Online]. Available: http://www.mead-usa.com/products/detail.aspx?id=4, accessed May 2008.

[14] All Sensors Corporation, "Miniature amplified low pressure sensors," [Online]. Available: http://www.allsensors.com/datasheets/industrial_temp/min_amp_low_prime.pdf, accessed May 2008.

[15] "Federal motor vehicle safety standard no.121: Air brake systems," Code of Federal Regulations, Title 49, Part 571, Section 121.

[16] M. Saad, *Compressible Fluid Flow 2nd ed.*, Prentice-Hall Inc., Englewood Cliffs, New Jersey, 1993.

[17] M. Nyberg and A. Perkovic, "Model based diagnosis of leaks in the air-intake system of an SI-engine," *SAE spec publ*, vol. 1357, pp. 25–31, 1998.

[18] National Instruments, "PCI E series user manual:multifunction I/O devices for PCI bus computers," [Online]. Available: http://www.ni.com/pdf/manuals/370503k.pdf, accessed May 2008.

[19] University of Sydney, "Aerodynamics for students," [Online]. Available: http://www-mdp.eng.cam.ac.uk/library/enginfo/aerothermal_dvd_only/aero/fprops/pipeflow/node22.html, accessed May 2008.

[20] R.W. Miller, *Flow Measurement Engineering Handbook*, McGraw-Hill Professional, New York, 1996.

[21] McMaster-Carr, "Flow control orifices, catalog p471," [Online]. Available: http://www.mcmaster.com/, accessed May 2008.

VITA

Srivatsan Ramarathnam was born in the city of Chennai, in southern part of India. He was brought up in the town of Ranipet and completed high school there. He obtained his Bachelor of Engineering in mechanical engineering from PSG College of Technology, Coimbatore, India in May 2003. He joined Ashok Leyland Ltd, the second largest commercial vehicle manufacturer in India, as a Senior Development Engineer in the Product Development division in June 2003. He joined the Department of Mechanical Engineering at Texas A&M University in August 2005 to pursue his Master of Science in mechanical engineering and graduated with the same in August 2008. He may be contacted through Professor K. R. Rajagopal, Department of Mechanical Engineering, Texas A&M University, College Station, Texas 77843, USA.

The typist for this thesis was Srivatsan Ramarathnam.